Electronic Supplementary Material (ESI) for Journal of Materials Chemistry A.

Enhanced oxygen exchange capacity in nano-structured ceria–vanadia multi-phase oxygen carriers for solar thermal fuel production

Asim Riaz[a], Muhammad Umair Ali[b], Wojciech Lipiński[a,*], Adrian Lowe[a,**]

[a] Research School of Electrical, Energy and Materials Engineering, The Australian National University, Canberra, ACT 2601, Australia.

[b] Department of Materials Science and Engineering, College of Engineering, Peking University, Beijing 100871, China

[*] Corresponding author. *E-mail*: wojciech.lipinski@anu.edu.au; *Tel*: +61 2 612 57896

[**] Corresponding author. *E-mail*: adrian.lowe@anu.edu.au; *Tel*: +61 2 612 54881.

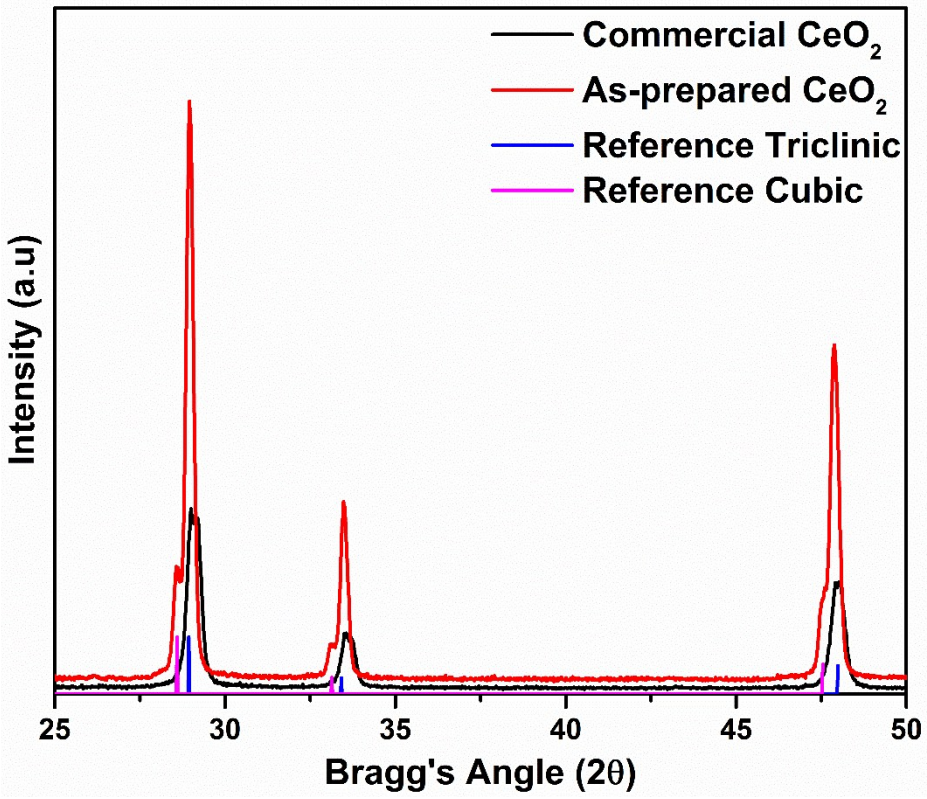

S 1. Structural comparison of different CeO_2 structures: (red) XRD pattern of as-prepared CeO_2 representing a triclinic (COD ID: 96-721-7888) with a low angle shoulder cubic (COD ID: 96-434-3162); (black) XRD pattern of commercial CeO_2 powder purchased from Sigma. Reference patterns are obtained from crystallographic open database (COD).

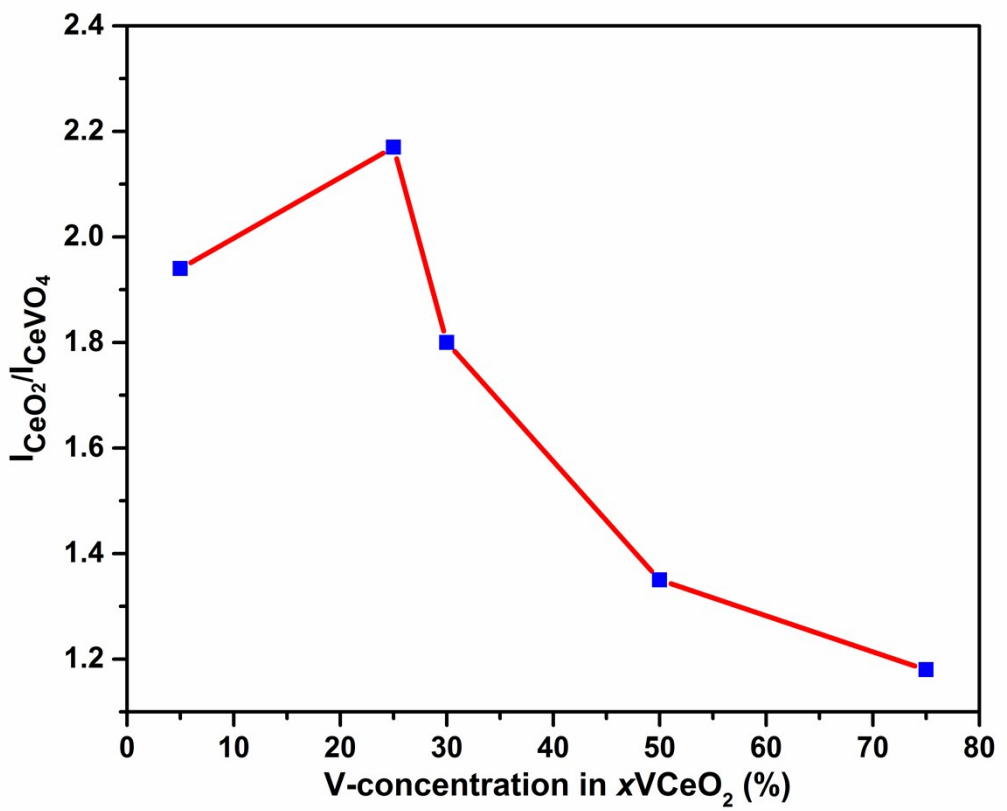

S 2. XRD peak Intensity ratios of $CeO_2/CeVO_4$ representing the phase segregation of CeO_2 and $CeVO_4$ in xVCeO$_2$ (x=5-75%).

Methane conversion

T 1. Methane conversion (X_{CH4}) by pure ceria and CV25 samples during MPO–CDS, MPO–WS, MPO–WS–CDS and MPO–CDS–WS redox cycles

Process	Materials	
	Ceria	CV25
MPO–CDS	0.1158	0.12
MPO–WS	0.034	0.072
MPO–WS–CDS	0.059	0.09
MPO–CDS–WS	0.0323	0.077

Methane conversion was calculated by:

$$\boldsymbol{X}\mathbf{CH_4} = \frac{\boldsymbol{n}_{\mathbf{CH_4,IN}} - \boldsymbol{n}_{\mathbf{CH_4,OUT}}}{\boldsymbol{n}_{\mathbf{CH_4,IN}}} \quad \text{(E1)}$$

$n_{CH_4,IN}$ and $n_{CH_4,OUT}$ are the number of moles of Methane going into and out from the reactor

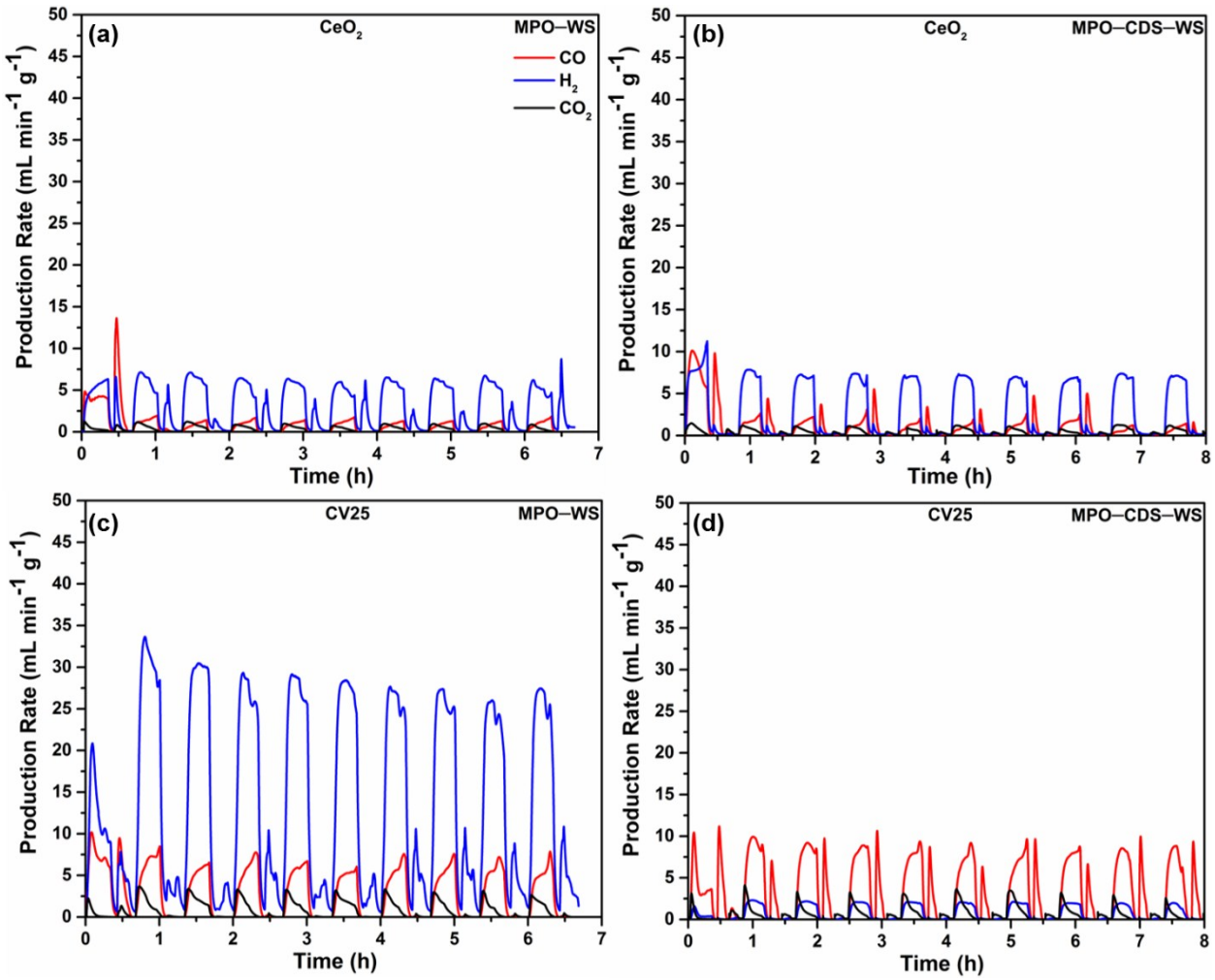

S 3. Production rates of H_2 (blue), CO (red) and CO_2 (black) during: (a) MPO–WS and (b) MPO–CDS–WS on pure nano-structured ceria; (c) MPO–WS and (d) MPO–CDS–WS on CV25. High CO_2 production rates relative to the CO rates are presented in MPO–WS cycles. MPO–CDS–WS represents incomplete oxidation of methane, resulting high H_2 rates.

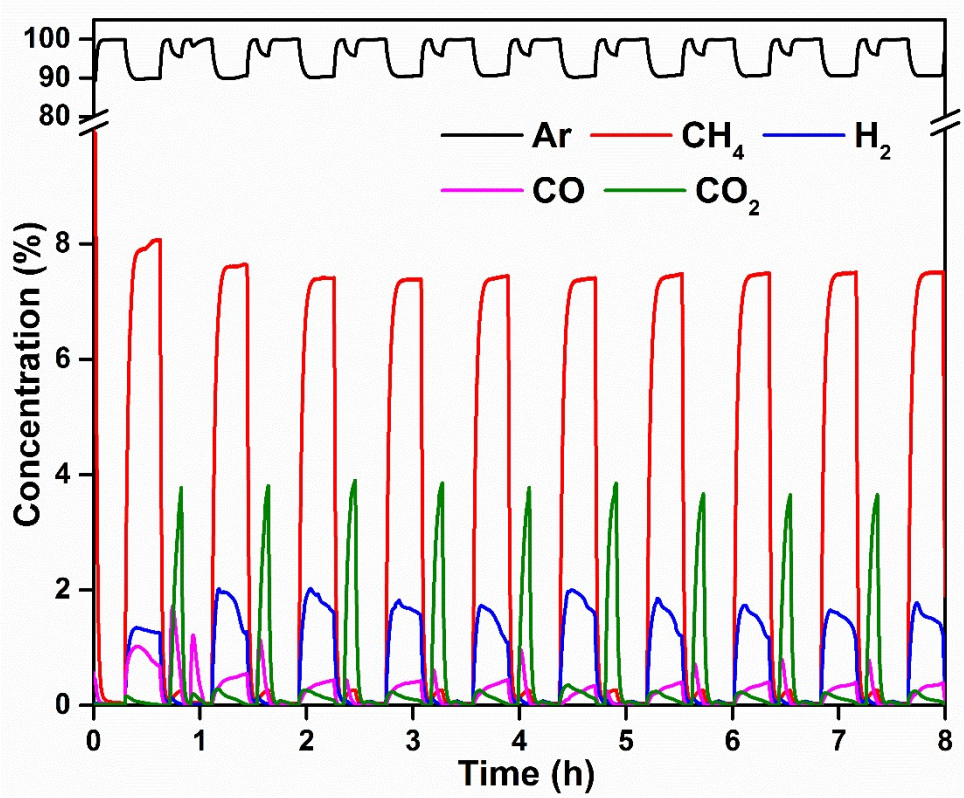

S 4. Real-time reactant and product gas production profiles measured by mass-spectrometer during MPO–WS–CDS redox cycles.

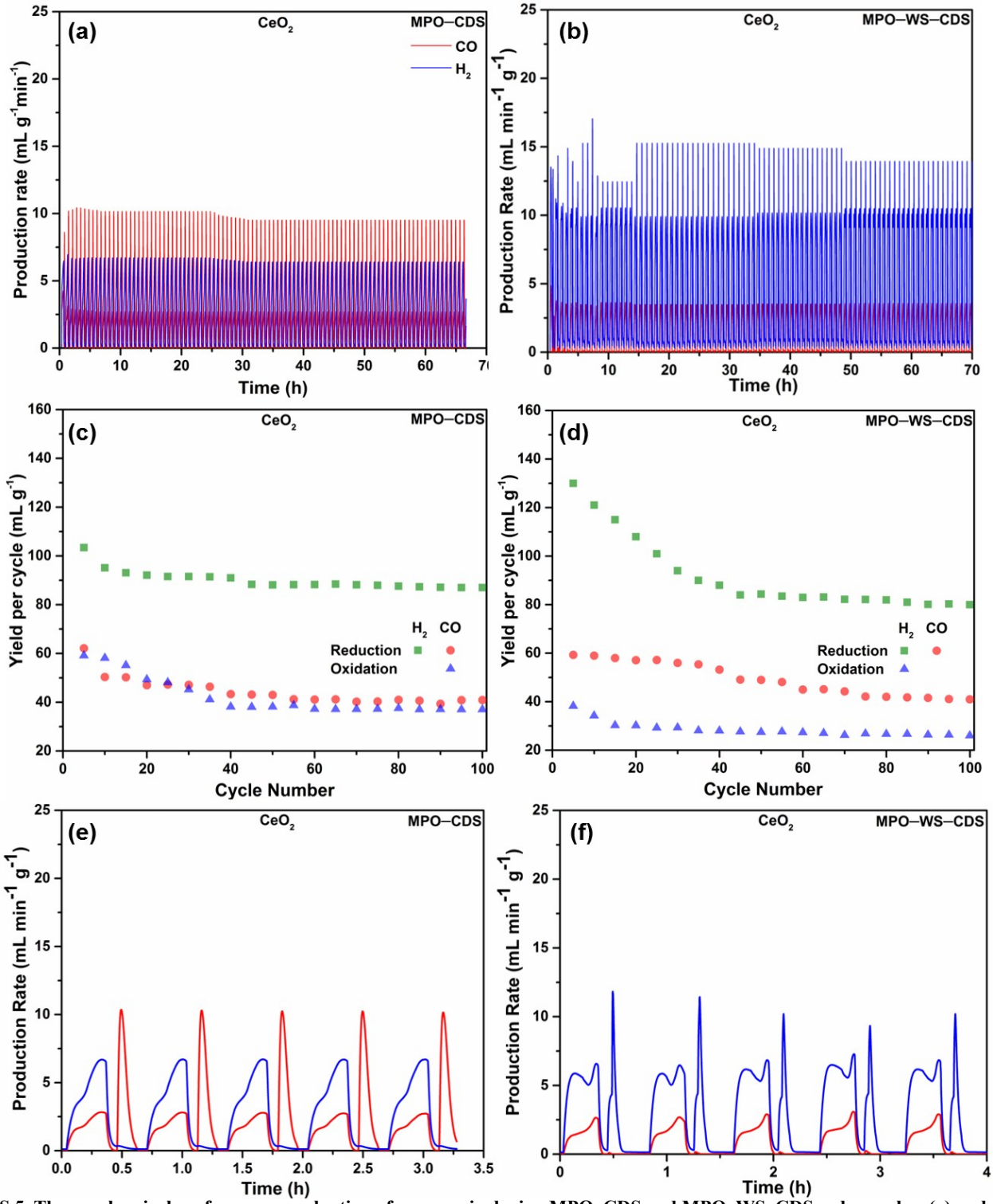

S 5. Thermochemical performance evaluation of nano-ceria during MPO–CDS and MPO–WS–CDS redox cycles: (a) and (b) H_2 and CO production rates; (c) and (d) average yield per 5 cycles; (e) and (f) 5 post 100 cycles.

Table T2. Performance evaluation of pure ceria and CV25 samples in terms of H_2/CO ratio, CO selectivity and fuel yield during oxidation and reduction steps of MPO–CDS and MPO–WS cycles.

		MPO–CDS					MPO–WS				
		Reduction				Oxidation	Reduction				Oxidation
Material	**Cycle (#)**	**H_2 yield (mL g^{-1}_{MO})**	**CO yield (mL g^{-1}_{MO})**	**SCO (%)**	**H_2/CO**	**CO yield (mL g^{-1}_{MO})**	**H_2 yield (mL g^{-1}_{MO}**	**CO yield (mL g^{-1}_{MO})**	**SCO (%)**	**H_2/CO**	**H_2 yield (mL g^{-1}_{MO})**
CeO_2	2	78.27	39.12	66.52	2.01	42.47	107.1	26.11	89.59	4.1	21.62
	4	68.4	37.4	59.06	1.83	43.2	93.8	19.1	87.1	4.92	20.1
	6	59.9	33.8	50.55	1.77	38.8	78.2	19.9	59.26	3.93	23.2
	8	51.58	29.14	76.8	1.78	34.49	78.62	14.52	36.74	5.87	19.15
	10	43.9	26.2	49.6	1.73	23.7	65.8	15.7	24.15	4.17	23.3
CV25	2	157	94.9	86.03	1.95	82.6	520	117	84.96	4.46	32.4
	4	128.34	74.51	85.35	2.12	65.39	477.92	112.45	77.92	4.25	51.522
	6	120.8	71.72	78.29	2.15	56.82	417.57	132.98	74.5	3.14	26.45
	8	114	65.91	83.75	2.22	43.75	389.2	152	67.69	2.56	67.04
	10	109.19	62.39	90.14	2.18	39.85	344.02	131.06	63.25	2.52	71.69

Table T3. Performance evaluation of pure ceria and CV25 samples in terms of H_2/CO ratio, CO selectivity and fuel yield during oxidation and reduction steps of MPO–WS–CDS and MPO–CDS–WS cycles.

		MPO–WS–CDS					MPO–CDS–WS				
		Reduction				Oxidation	Reduction				Oxidation
Material	**Cycle (#)**	**H_2 yield** ($mL\ g^{-1}_{MO}$)	**CO yield** ($mL\ g^{-1}_{MO}$)	**SCO (%)**	**H_2/CO**	**H2 yield** ($mL\ g^{-1}_{MO}$)	**H_2 yield** ($mL\ g^{-1}_{MO}$)	**CO yield** ($mL\ g^{-1}_{MO}$)	**SCO (%)**	**H_2/CO**	**CO yield** ($mL\ g^{-1}_{MO}$)
CeO_2	2	112.27	56.01	88.38	2.01	50.26	131.62	32.05	87.73	4.1	17.91
	4	84.8	46.42	88.4	1.82	16.66	112.3	22.49	85.7	4.99	19.49
	6	70.34	33.13	88	2.23	14.23	102.5	16.27	71.4	6.29	9.48
	8	58.14	32.17	84.95	1.75	20.36	82.82	27.54	42.16	3	7.92
	10	54.68	27.6	84.8	1.98	29.09	79.5	13.07	27.8	6.08	6.85
CV25	2	171.2	65.38	92.8	3.16	54.5	161.25	34.28	94.2	4.7	27.41
	4	153.48	54.19	92.2	2.32	42.78	142.87	29.33	88.49	4.87	30.35
	6	138.26	51.84	90.29	2.29	36.52	116.51	25.81	55.1	4.38	17.7
	8	125.78	48.66	90.13	2.41	36.52	121.39	27.98	37.43	4.45	31.14
	10	109.16	46.12	89.89	2.37	34.15	138.81	31.47	26.3	4.41	18.72

Selectivity of CO during the MPO steps were calculated by:

$$\boldsymbol{S}(\mathbf{CO}) = \frac{\boldsymbol{n}(\mathbf{CO})_{\mathbf{MPO}}}{\boldsymbol{n}(\mathbf{CO})_{\mathbf{MPO}} + \boldsymbol{n}(\mathbf{CO_2})_{\mathbf{MPO}}} \times 100\% \qquad \text{(E2)}$$

$n(i)_{\mathrm{MPO}}$ denotes the total amount of evolution of species "i" during MPO steps.